Supplemental online material

Investigation of bound and unbound phosphoserine phosphatase conformations through Elastic Network Models and Molecular Dynamics simulations

Laurence Leherte, Marie Haufroid, Manon Mirgaux, Johan Wouters

Laboratoire de Chimie Biologique Structurale, Unité de Chimie Physique Théorique et Structurale, Department of Chemistry, NAmur Research Institute for LIfe Sciences (NARILIS), NAmur MEdicine & Drug Innovation Center (NAMEDIC), Namur Institute of Structured Matter (NISM), University of Namur, Rue de Bruxelles 61, B-5000 Namur (Belgium)

S1. Ligand and enzyme structure building

Starting from the crystal structure coordinates of phosphoserine (PSer), hydrogen atoms were added with VegaZZ (Pedretti et al., 2004). The resulting structure was then grossly optimised using the steepest descent algorithm of VegaZZ with a tolerance of 1.0 $kcal.mol^{-1}.Å^{-1}$, a high value selected to prevent any drastic modification of the heavy atoms coordinates. Gromacs coordinates and topology files were generated using Topolbuild (Ray, 2009). Parameters reported in references (Homeyer et al., 2006; Steinbrecher et al., 2012) were considered so as to retain a conformational degeneracy of the three phosphate oxygen atoms. All three P-O distances were kept identical.

The atomic charges of PSer were determined using the Quantum Mechanics program Gaussian (Frisch et al., 2009) at the RHF/6-31G(d) level, a molecular electrostatic potential (MEP) grid of 250 x 250 x 250 elements and a grid interval of 0.1 Å was generated according to the Merz-Singh-Kollman scheme (Singh & Kollman, 1984; Besler et al., 1990). A modified version of QFIT (Borodin & Smith, 2009) was run to determine the atomic charges (Table S1). The program code was adapted so as to fit electrostatic forces calculated from electrostatic potential grids, as described in Ref. (Leherte, 2016).

Table S1. RHF/6-31G(d) atomic charges ($|e^-|$) of PSer obtained using Gaussian (Frisch et al., 2009).

Atom	Net charge	Atom	Net charge
N	-0.8460	CB	0.0728
H1, H2, H3	0.4196	HB1, HB2	0.0471
CA	0.1600	OG	-0.5204
HA	0.0178	OXT	-0.8163
C	0.8860	O1P, O2P, O3P	-0.9962
O	-0.8163	P	1.4980

From the reference MEP grids, fittings were achieved by considering points located at distances between 1.4 and 2.0 times the van der Waals radius of the atoms. These two limiting distance values were selected after the so-called Merz-Singh-Kollman scheme (Singh & Kollman, 1984). Constraints, such as the total molecular charge (-2 $|e^-|$) and the total dipole moment were applied. Additional constraints were considered so as to force the atomic charges of the atoms H1, H2, and H3, to be equal, as well as for atoms HB1 and HB2, and O1P, O2P, and O3P.

Regarding the protein, the missing three first amino acid residues of chainA, Met1-Ile2-Ser3, were added using the following procedure. First, chain B, which contains the first three residues, was aligned onto chain A. The residue coordinates were saved and added to the incomplete chain A. The chain B of hPSP-PSer was selected to model the open form of the enzyme. The missing amino acid side chains of residues 47 to 50 were generated using the web server BetaSCPWeb (Ryu et al., 2016). Both enzyme structures were protonated using the standard protonation states of the amino acid residues, i.e., charged end residues, positive Lys and Arg, and negative Glu and Asp.

S2. Molecular Dynamics simulations

MD trajectories of the solvated systems were run using the Gromacs 4.5.5 program package (Hess et al., 2008; Pronk et al., 2013) with the Amber99sb-ildn FF (Lindorff-Larsen et al., 2010) under particle mesh Ewald (PME) periodic boundary conditions and a Coulomb cut-off distance of 1.0 nm. The ligand PSer was described using the Amber Force Field parameters reported in (Homeyer et al., 2006; Steinbrecher et al., 2012). The Newton equations of motion were numerically integrated using a leap-frog integrator. The van der Waals cut-off distance was set equal to 1.2 nm. Long-range dispersion corrections to energy and pressure were applied. The systems were optimised using a steepest descent algorithm with an initial step size of 0.10 nm. To strongly reduce the calculation time, the hybrid TIP3P/SIRAH water FF was used (Darré et al., 2012; Gonzáles et al., 2013; Darré et al., 2015). The initial protein systems (with and without ligand) were solvated so as protein atoms lie at least at a distance of 2.0 nm from the cubic box walls. A shell of 1.0 nm thickness of TIP3P water molecules was defined around the protein complex, and the remaining space of the solvation box was filled with SIRAH water beads (Machado et al., 2018) where each bead is composed of four interaction sites and represents about 11 water molecules. A mix of SIRAH Na^+ and K^+ ions were added to cancel the electric charge of the systems.

Various MD simulations were carried out (Figure 2 and Table S2).

Table S2. Description of the protein systems simulated using Gromacs at T = 300 K, and at P = 1 bar in hybrid TIP3P/SIRAH water.

	Total no. of particles	No. of all-atom/CG water molecules	Total no. of ions	Final box size (nm)
Chain A – based MD				
A/Ca/PSer	25,202	3,372/2,883	3 K^+, 2 Na^+	10.36499
A_w/Ca/PSer	25,556	3,502/2,874	3 K^+, 2 Na^+	10.37705
A/Mg/PSer	25,202	3,372/2,883	3 K^+, 2 Na^+	10.35826
A_c/Mg/PSer	25,202	3,372/2,883	3 K^+, 2 Na^+	10.35826
A_{cw}/Mg/PSer	25,556	3,502/2,874	3 K^+, 2 Na^+	10.36459
A_c/Mg	25,183	3,372/2,883	3 K^+	10.37098
A_{cw}/Mg	25,537	3,502/2,874	3 K^+	10.38672
Chain B – based MD				
B/Ca	26,886	3,709/3,056	3 K^+	10.56515
B/Mg	26,886	3,709/3,056	3 K^+	10.57560
B/Ca/PSer	26,887	3,707/3,053	3 K^+, 2 Na^+	10.56797
B/Mg/PSer	26,887	3,707/3,053	3 K^+, 2 Na^+	10.56653

In simulations A/Ca/PSer and A/Mg/PSer, a calcium (or magnesium) ion was considered at the crystallographic position of Ca^{++} in the active site. Crystallographic water molecules were added in simulation A_w/Ca/PSer to generate a second starting configuration of the system involving PSer and Ca^{++}. Among the crystallographic water, 101 molecules were selected according to their proximity of the PSer/hPSP structures. The final conformations of the systems A/Ca/PSer and A_w/Ca/PSer were used as starting points for the simulations of magnesium-dependent systems, named A_c/Mg/PSer and A_{cw}/Mg/PSer. The last frame of these two simulations were themselves used as starting configurations of substrate-free systems, named A_c/Mg and A_{cw}/Mg, respectively.

Simulations of the open chain B were achieved considering calcium and magnesium metal ions, with and without the substrate PSer.

The whole systems were again optimised to eliminate large forces, using a steepest descent algorithm with an initial step size of 0.10 nm, and then heated to 50 K through a 10 ps canonical (NVT)

MD, with a time step of 2 fs and LINCS constraints acting on bonds involving H atoms. The trajectory was followed by two successive 20 ps heating stages, at 150 K and at the final temperature of 300 K, under the same conditions. Next, each system was equilibrated during 50 ps in the NPT ensemble, at P = 1 bar, to relax the solvent molecules, and for a further 60 ns MD equilibration run. The 'V-Rescale' and 'Parrinello-Rahman' algorithms were selected to constrain T and P, respectively. A final run of 300 ns (150 x 10^6 steps) was performed for the evaluation of the structural, energetics, and dynamical properties of each system. Trajectory data were saved every 20 ps.

Only the last 200 ns of that final run were used as the production stage to eliminate the most fluctuating part of the trajectories. Consequently, the equilibration stage duration is equal to 160 ns.

Table S3. ED parameters $w'_{a,i}$ (no unit) and $\zeta'_{a,i}$ (bohr^{-2}) coefficients as obtained to fit the Cromer-Mann parameters. The mathematical relationships and the parameter values for the atom types C, N, O, and S are given in (Leherte, 2004).

	H	P	Ca^{++}	Mg^{++}
w_1'	0.16854600	0.46415333	0.10788983	0.28236667
ζ_1'	1.56469094	3.03261175	3.75576265	2.63869650
w_2'	0.56040540	0.27319333	0.33417363	0.33042500
ζ_2'	0.46127543	0.20714039	15.7577288	1.18568426
w_3'	0.00537593	0.15659333	0.42716802	0.14668333
ζ_3'	20.2478100	34.0072686	0.53608875	47.8823755
w_4'	0.26525298	0.10598000	0.03239855	0.07385417
ζ_4'	0.16430279	0.08324861	0.21165146	0.55016835

Table S4. First three eigenvalues (nm^2) obtained from the PCA of hPSP as obtained from the last 200 ns of MD trajectories at 300 K and 1 bar.

	λ_1	λ_2	λ_3
Chain A			
A/Ca/PSer	1.110	0.469	0.221
A_w/Ca/PSer	0.925	0.255	0.168
A_c/Mg/PSer	0.783	0.352	0.169
A_{cw}/Mg/PSer	0.652	0.186	0.139
A/Mg/PSer	0.726	0.371	0.095
A_c/Mg	0.415	0.287	0.191
A_{cw}/Mg	0.598	0.267	0.173
Chain B			
B/Ca	0.521	0.322	0.207
B/Mg	0.455	0.275	0.264
B/Ca/PSer	0.855	0.185	0.132
B/Mg/PSer	0.602	0.306	0.197

Table S5. Cation coordination with oxygen atoms as reported from experiments (Peerear et al., 2004; Haufroid et al., 2019) and the last 200 ns of MD simulations at 300 K and 1 bar. A cutoff value of 0.25 and 0.35 nm is used when Mg^{++} and Ca^{++} are considered, respectively. Integration under the first peak of the radial distribution functions g(ion-oxygen) is given in parentheses

Magnesium-dependent hPSP (Peerear et al., 2004) Asp20 (OD1) Asp22 (O) Asp179 (OD2) Three H_2O	*Calcium-dependent hPSP* (Peerear et al., 2004) Asp20 (OD1, OD2) Asp22 (O) Asp179 (OD2) Three H_2O
(Haufroid et al., 2019) Asp20 (OD1, OD2) – 0.311 and 0.225 nm Asp22 (O) – 0.231 nm Asp179 (OD1, OD2) – 0.218 and 0.342 nm Three H_2O – 0.224, 0.242, 0.242 nm	
A/Ca/PSer (8.2) – Figure 7b Asp20 (partly OD1, OD2) Asp22 (O, OD1) Asp179 (OD1) Asp183 (OD1, OD2) PSer (O) Exchangeable H_2O	*A_w/Ca/PSer (8.6)* – Figure 7a Asp20 (OD1, OD2) Asp22 (O) Asp179 (OD1) Asp183 (OD1, OD2) PSer (O1P in a less extent, O2P, O3P)
A_c/Mg/PSer (5.7) Asp20 (OD2) Asp22 (OD2) Asp179 (OD1) Asp183 (OD1, OD2) PSer (O)	*A_{cw}/Mg/PSer (6.0)* Asp20 (OD2) Asp179 (OD1) Asp183 (OD2) PSer (O1P, O2P, O3P)
A/Mg/PSer (6.0) – Figure 7d Asp20 (OD1, OD2) Asp22 (O) Asp179 (OD1) Two permanent water molecules	
A_c/Mg (6.0) Asp20 (OD1, OD2) Asp22 (O, OD2) Asp179 (OD1) Asp183 (OD1)	*A_{cw}/Mg (6.0)* Asp20 (OD2) Asp22 (O) Asp179 (OD1) Asp183 (OD2) Two permanent water molecules
B/Ca (8.9) Asp20 (OD2) Asp22 (O) Asp179 (OD1, OD2) Asp183 (OD1, OD2) Non-permanent water molecules	*B/Mg (6.0)* Asp20 (OD2) Asp22 (O) Asp179 (OD1, OD2) Asp183 (OD2) One permanent water molecule
B/Ca/PSer (8.0) – Figure 7c Asp20 (OD2) Asp179 (OD1) Asp183 (OD1, OD2) PSer (O, O2P, O3P) One permanent water molecule	*B/Mg/PSer (6.0)* Asp20 (OD2) Asp179 (OD1) Asp183 (OD2) PSer (O1P, O2P, O3P)

Table S6. RMSF (nm) of coordinated oxygen atoms (Table S5) as obtained from the last 200 ns of MD simulations at 300 K and 1 bar.

	Total	Asp	PSer	H_2O
A/Ca/PSer	1.51 ± 1.12	0.95 ± 0.07	3.80	/
A_w/Ca/PSer	2.12 ± 0.75	1.59 ± 0.06	1.59 ± 0.06	/
A_c/Mg/PSer	1.35 ± 0.61	0.95 ± 0.02	/	1.82, 2.50
A_{cw}/Mg/PSer	0.11 ± 0.05	0.12 ± 0.06	0.07	/
A/Mg/PSer	0.15 ± 0.04	0.18 ± 0.04	0.12 ± 0.000(9)	/
A_c/Mg	0.03 ± 0.01	0.03 ± 0.01	/	/
A_{cw}/Mg	0.01 ± 0.000(6)	0.01 ± 0.000(8)	/	0.011, 0.011
B/Ca	0.06 ± 0.03	0.06 ± 0.03	/	/
B/Mg	1.11 ± 0.99	0.67 ± 0.05	/	3.31
B/Ca/PSer	2.48 ± 0.10	2.48 ± 0.10	2.46 ± 0.09	2.55
B/Mg/PSer	0.01 ± 0.000(7)	0.01 ± 0.000(2)	0.01 ± 0.000(9)	/

Table S7. Occurrence frequency (> 20 %) and hydrogen bonds formed by of water molecules in contact (d ≤ 0.4 nm) with residues Asp179, Phe196, Gly197, and Val200 to Arg202, as obtained from the last 200 ns of MD trajectories at 300 K and 1 bar.

	Occurrence frequency	Hbonds formed with
A/Ca/PSer	100	Asp179, Val200, Arg202
	100	Phe196, Val200
A_w/Ca/PSer	100	Asp179, Phe196, Val200, Arg202
	98	Phe196, Val200
A_c/Mg/PSer	69	Phe196, Val200
	52[a]	Asp179, Phe196, Val200, Arg202
	41[b]	Asp179, Phe196, Val200, Arg202
	21[c]	Asp179, Phe196, Val200, Arg202[d]
	21[e]	Asp179, Phe196, Val200, Arg202
A_{cw}/Mg/PSer	64	Asp179[f], Phe196[f], Val200[f], Arg202[f]
	64	Phe196[g], Val200[g]
	32	Asp179, Phe196[h], Val200[h], Arg202[h]
A/Mg/PSer	100	Asp179, Val200, Arg202
	76	Phe196, Val200
A_c/Mg	76	Phe196, Val200
	67[i]	Asp179, Phe196, Val200, Arg202
A_{cw}/Mg	81[j]	Asp179, Phe196, Val200, Arg202
	48[k]	Phe196, Val200
	40[l]	Phe196, Val200
B/Ca	97	Phe196, Val200
	93	Asp179, Phe196, Val200, Arg202
	33[m]	Asp179, Phe196, Val200, Arg202
B/Mg	80	Phe196, Val200
B/Ca/PSer	27[n]	Asp179, Phe196
B/Mg/PSer	100	Phe196, Val200
	52[o]	Asp179, Phe196, Val200, Arg202
	28[o]	Asp179, Phe196, Val200, Arg202
	21[o]	Asp179, Phe196, Val200, Arg202

[a] 100-202 ns; [b] 202-300 ns; [c] 166-210 ns; [d] 210-238 ns; [e] 220-271 ns; [f] After 157 ns; [g] After 130 ns; [h] After 205 ns; [i] 100-234 ns; [j] 100 to 262 ns; [k] 100 to 205 ns; [l] from 205 ns; [m] 230-300 ns; [n] 190-300 ns; [o] Three exchanging water molecules at a single site.

Table S8. Mean short-range interaction energy and standard deviation (kJ/mol) as obtained from the last 200 ns of MD simulations at 300 K and 1 bar.

	Cation-H_2O	Cation-PSer	hPSP-PSer
A/Ca/PSer	-21.76 ± 51.76	-190.54 ± 29,80	-381.53 ± 56.94
A_w/Ca/PSer	125.62 ± 45.85	-515.65 ± 62.58	-122.43 ± 68.13
A_c/Mg/PSer	135.54 ± 35.11	-412.73 ± 100.91	-615.48 ± 101.31
A_{cw}/Mg/PSer	274.20 ± 34.62	-1386.35 ± 34.50	155.67 ± 75.93
A/Mg/PSer	-405.29 ± 32.13	-117.97 ± 26.34	-294.65 ± 55.05
A_c/Mg	139.21 ± 82.29	/	/
A_{cw}/Mg	-423.70 ± 34.00	/	/
B/Ca	-272.91 ± 74.55	/	/
B/Mg	-195.07 ± 31.90	/	/
B/Ca/PSer	70.18 ± 30.43	-629.55 ± 26.54	-291.47 ± 43.94
B/Mg/PSer	286.69 ± 34.75	-1389.37 ± 35.59	171.70 ± 57.35

Table S9. Most frequent PSer-hPSP Hbond types as obtained from the last 200 ns of MD simulations at 300 K and 1 bar. The ligand orientation is described using the PSer group in interaction with the metal ion.

	PSer-hPSP Hbond type	Ligand orientation
A/Ca/PSer	nh3-Glu29 po3-Arg65 O-Lys158, Thr182	coo-metal
A_w/Ca/PSer	nh3-Glu29, Asp179 po3-Ser23, Lys158 O-Gly53	po3-metal
A_c/Mg/PSer	nh3-Asp22, Glu29 po3-Arg50, Arg65, Arg202 O-Lys158	coo-metal
A_{cw}/Mg/PSer	nh3-Glu29 po3-Lys158 O-Arg49, Gly53	po3-metal
A/Mg/PSer	nh3-Glu29 po3-Lys158, Thr182 O-Arg202	screened po3-metal
B/Ca/PSer	nh3-Asp22, Glu29 po3-Arg49, Lys158	bridged
B/Mg/PSer	po3-Lys158 O-Thr48, Arg49	po3-metal

Table S10. Intermolecular passes (located at a distance ≤ 0.3 nm from PSer) detected in the optimised crystal structure and in the last frame of the MD trajectories of the PSer-hPSP complexes as obtained from a topological analysis of the Cromer-Mann based promolecular ED distribution function. SR interaction energy value are given for pairs PSer - residue of hPSP. Hbonds and salt bridges (bold) are identified using VMD (Humphrey et al.,1996) and PLIP (Salentin et al., 2015).

PSer atom	hPSP atom	ρ (e/bohr^3)	e2 (e/bohr^5)	Energy (kJ/mol)
Optimised crystal structure				
HA	Ala51(O)	0.0092	-0.0085	-2.27
O2P	**Gly110(H)**	**0.0273**	**-0.0293**	-57.51
O1P	Gly110(HA1)	0.0096	-0.0021	
OXT	Gly180(HA)	0.0021	-0.0014	-16.59
O	**Gly53(H)**	**0.0400**	**-0.0555**	-30.34
O1P	Lys158(HE1)	0.0099	-0.0015	-156.51
O2P	**Lys158(HZ1)**	**0.0232**	**-0.0246**	
OG	Lys158(HZ2)	0.0124	-0.0082	
CA	Met52(S)	0.0085	-0.0024	-17.37
HA	Met52(HA)	0.0090	-0.0055	
OXT	Met52(S)	0.0102	-0.0049	
O3P	Phe58(CE1)	0.0070	-0.0009	-11.60
HB2	Phe58(HE1)	0.0063	-0.0028	
O	**Thr182(HG1)**	**0.0548**	**-0.0813**	-58.53
HB1	Thr182(HG1)	0.0102	-0.0022	
HB1	Thr182(HG21)	0.0114	-0.0091	
A/Ca/PSer				
O	**Arg202(HH21)**	**0.0362**	**-0.0467**	-56.52
O3P	Arg50(HB2)	0.0005	-0.0004	-3.30
HB2	Arg50(O)	0.0003	-0.0002	
O2P	**Arg65(HH12)**	**0.0240**	**-0.0297**	-171.72
O3P	**Arg65(HH22)**	**0.0214**	**-0.0247**	
O	Asp179(OD2)	0.0065	-0.0035	66.60
carboxylate	cation	0.0121	-0.0093	-314.87
carboxylate	cation	0.0109	-0.0040	
O3P	Gly53(HA2)	0.0024	-0.0007	13.36
O	**Ser23(HB2)**	**0.0049**	**-0.0034**	-13.04
HB1	Thr182(O-H)	0.0051	-0.0013	-41.70
OXT	**Thr182(HG1)**	**0.0211**	**-0.0254**	
OG	**Thr182(HG23)**	**0.0042**	**-0.0017**	
H1	**Asp22(OD2)**	**(*)**		16.71
H2	**Glu29(OE2)**	**(*)**		-62.54
A_w/Ca/PSer				
O	**Arg202(HH22)**	**0.0135**	**-0.0075**	-56.95
HA	Arg65(HH22)	0.0042	-0.0018	7.07
O1P	Asp22(HB2)	0.0011	-0.0004	27.35
O1P	Asp22(O)	0.0017	-0.0006	
O1P	cation	0.0131	-0.0109	-588.07
O2P	cation	0.0109	-0.0048	
O3P	Gly180(HA1)	0.0021	-0.0016	-17.17
HB2	Gly53(HA1)	0.0002	-0.0001	-4.23
O2P	**Lys158(HZ2)**	**0.0280**	**-0.0343**	-121.60
NH3	**Ser23(HG)**	**0.0032**	**-0.0015**	-9.97
phosphate	Thr182(O-H)	0.0015	-0.0004	-5.76
O	Thr48(HG22)	0.0057	-0.0031	-2.73
H3	**Glu29(OE1)**	**(*)**		-130.09
A_c/Mg/PSer				
CB	Ala61(HB2)	0.0042	-0.0009	-14.25
OG	Ala61(O)	0.0053	-0.002	
O3P	**Arg202(H12)**	**0.0366**	**-0.0478**	-201.40
O2P	**Arg202(H22)**	**0.0308**	**-0.0385**	
O2P	**Arg50(H12)**	**0.0426**	**-0.0577**	-213.72
O1P	**Arg50(H22)**	**0.0307**	**-0.0397**	
O2P	**Arg65(H12)**	**0.031**	**-0.0361**	-183.01
O1P	**Arg65(H22)**	**0.0289**	**-0.0313**	
O	Asp22(OD2)	0.0127	-0.0064	2.91
H3	**Asp22(OD1)**	**0.0012**	**-0.0000**	
O	cation	0.0404	-0.0774	-435.88
H1	Glu29(OE1)	0.0276	-0.0285	-90.48
H2	Gly111(H)	0.0002	-0.0001	1.39

OXT	**Lys158(HZ1)**	**0.0383**	**-0.0513**	-108.65
carboxylate	Thr182(HB)	0.0064	-0.0021	-14.88
HB2	Thr182(HB)	0.0127	-0.0060	
O1P	Val56(H23)	0.0034	-0.0015	-4.26
A_{cw}/Mg/PSer				
OXT	**Arg202(NH1)**	**0.0008**	**-0.0002**	-10.47
H1	Arg202(NH2)	0.0039	-0.0008	
O	**Arg49(H12)**	**0.0246**	**-0.0300**	-138.59
OXT	**Arg49(H22)**	**0.0319**	**-0.0330**	
H1	Asp179(OE2)	0.0011	-0.0002	147.95
O1P	Asp183(OD1)	0.0048	-0.0008	154.31
O3P	cation	0.0421	-0.0588	-1308.53
O1P	cation	0.0358	-0.0345	
H2	**Glu29(OE1)**	**0.0165**	**-0.0145**	-43.66
O2P	**Gly180(HA1)**	**0.0036**	**-0.0024**	0.00(1)
O1P	**Lys158(HZ1)**	**0.0159**	**-0.0113**	-124.72
P	**Thr182(O-H)**	**0.0056**	**-0.0022**	-24.61
A/Mg/PSer				
OXT	Ala51(HB3)	0.0008	-0.0005	-2.19
HA	Ala61(HB1)	0.0005	-0.0003	-2.94
O	**Arg202(HH22)**	**0.002**	**-0.001**	-35.91
H1	Glu29(HB1)	0.0012	-0.0004	40.02
H2	**Glu29(OE2)**	**0.0033**	**-0.0021**	
O	Glu29(OE2)	0.0028	-0.0003	
OXT	Gly53(HA2)	0.0055	-0.0032	-18.04
HB2	Gly53(O)	0.0092	-0.0028	
OG	Gly54(HA2)	0.0018	-0.0004	-10.89
O2P	**water(HW1520)**	**0.0551**	**-0.0858**	-67.17
O3P	**water(HW1534)**	**0.0341**	**-0.0443**	-34.59
H1	water(HW1534)	0.0101	-0.0063	
O1P	**Lys158(HZ1)**	**0.0293**	**-0.0329**	-229.15
O3P	**Lys158(HZ3)**	**0.0205**	**-0.0193**	
O1P	**Thr182(HB)**	**0.0035**	**-0.002**	-32.48
B/Ca/PSer				
OG	Arg49(CB group)	0.0039	-0.0005	-150.86
O1P	**Arg49(HH21)**	**0.0426**	**-0.0607**	
O1P	**Arg49(HE)**	**0.0187**	**-0.0106**	
O2P	**Arg50(HH12)**	**0.0281**	**-0.0354**	-113.42
HB1	Arg50(NH1)	0.0052	-0.0013	
OXT	Asp179(OD1)	0.0031	-0.0017	87.88
OXT	**Asp22(HB2)**	**0.0075**	**-0.0059**	-50.94
H3	**Asp22(OD2)**	**(*)**		
OXT	cation	0.0099	-0.0116	-595.61
O2P	cation	0.0075	-0.0058	
O3P	cation	0.0070	-0.0047	
O3P	Lys158(HZ3)	0.0214	-0.0180	-172.76
O1P	**Lys158(HZ3)**	**0.0187**	**-0.0126**	
O1P	**Thr182(HG1)**	**0.0321**	**-0.0334**	-67.23
O	Thr48(HG23)	0.0005	-0.0003	-6.77
HB1	Thr48(O)	0.0097	-0.0069	
B/Mg/PSer				
H3	Arg202(H22)	0.0007	-0.0002	-1.04
OXT	**Arg49(HH21)**	**0.0550**	**-0.0824**	-139.04
O	**Arg49(HE)**	**0.0241**	**-0.0271**	
O3P	cation	0.0311	-0.0343	-1335.30
P	cation	0.1399	-0.0768	
O1P	cation	0.0279	-0.0221	
O2P	cation	0.0308	-0.0342	
H1	Glu29(OE2)	0.0006	-0.0004	-12.77
O1P	**Lys158(HZ1)**	**0.0434**	**-0.0637**	-154.14
HB2	Phe58(CD1)	0.0012	-0.0004	
HA	Phe58(CE1)	0.0016	-0.0007	-12.76
O2P	**Thr182(O-H)**	**0.0065**	**-0.0017**	-25.92

(*) Hbond not seen as a CP but detected using isocontours of s(**r**)

Table S11. Long-living hydrogen bonds formed between residues 50-55 and 202-206 as obtained from the last 200 ns of the MD simulations at 300 K and 1 bar.

	Hbond type	duration from-to (ns)
A/Ca/PSer	/	/
A_w/Ca/PSer	Met52-Gln204	100-200
	Met52-Gly53	100-200
	Met52-Gly54	200-300
A_c/Mg/PSer	Met52-Gln204	150-265
	Ala51-Gln203	150-265
A_{cw}/Mg/PSer	/	
A/Mg/PSer	Met52-Gln204	190-300
A_c/Mg	Met52-Gln204	170-300
A_{cw}/Mg	/	
B/Ca	/	
B/Mg	/	
B/Ca/PSer	Arg50-Gln204	190-300 (rare)
B/Mg/PSer	/	

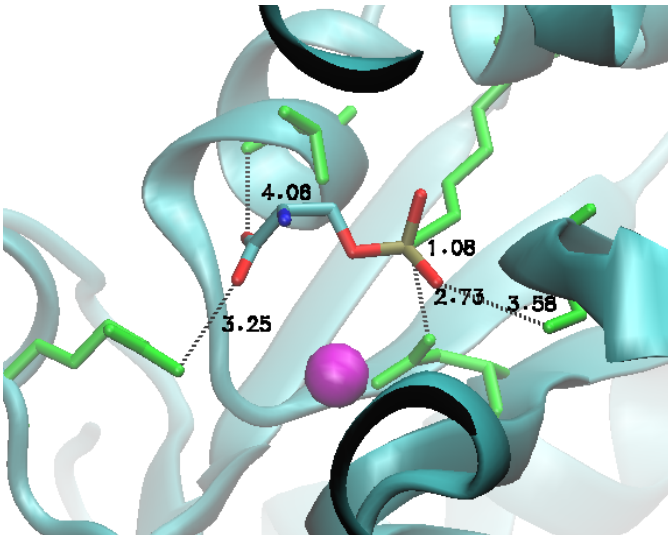

Figure S1. Crystal structure of the chain B showing close contacts between the artificially included substrate (sticks) and hPSP (cyan ribbon). Ca^{++} and the residues Asp20, Met52, Phe58, Lys158, and Thr182, are displayed in magenta and green, respectively. Distance values are in Angströms.

To place the substrate in Chain B, the crystal structure of Chain A and PSer was aligned onto the crystal structure of Chain B using the default alignment parameters of the program Pymol (Schrödinger, 2014). PSer is close to Lys158 (NZ-O2P = 0.11 nm), Asp20 (OD1-O2P = 0.27 nm), Arg202 (NH2-OXT = 0.33 nm), Ser109 (OG-O3P = 0.36 nm), and Lys182 (N-O = 0.41 nm).

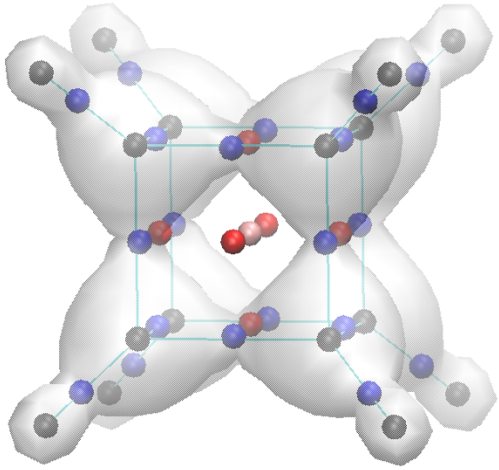

Figure S2. Critical points (peaks = black, passes = blue, pales = red, pit = pink) of the promolecular Cromer-Mann based electron density distribution for the cubane molecule (lines). The ED iso-contour value is 0.17 e/bohr^3 (light grey transparent contour).

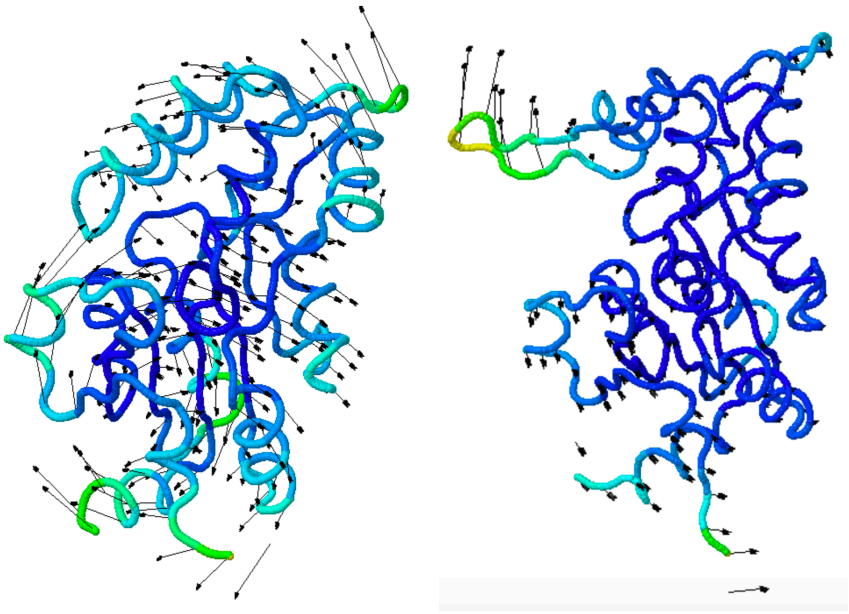

Chain A Chain B

Figure S3. Screenshots of the first vibrational mode of chains A and B of hPSP as obtained from the application of the server iMods (López-Blanco et al., 2014). The sequences are colour-coded as a function of their predicted deformability. The protein backbone colours are chosen according to the predicted mobility reported in Figure 3a.

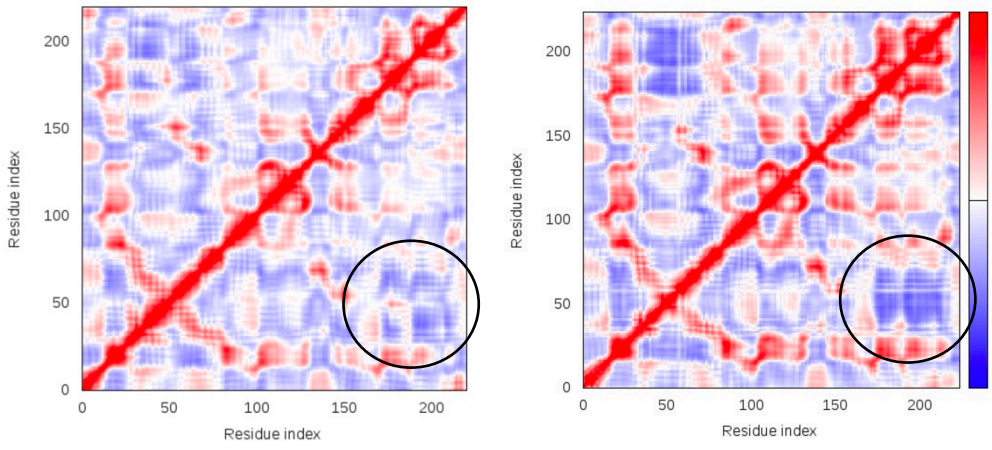

Chain A Chain B

Figure S4. Correlation matrices defined in Ref. (Ichiye & Karplus, 1991) (negative = blue, positive = red) computed using the Cα coordinates of the chains A and B of hPSP. The circles focus on the negative correlation region between both elements of the cavity aperture.

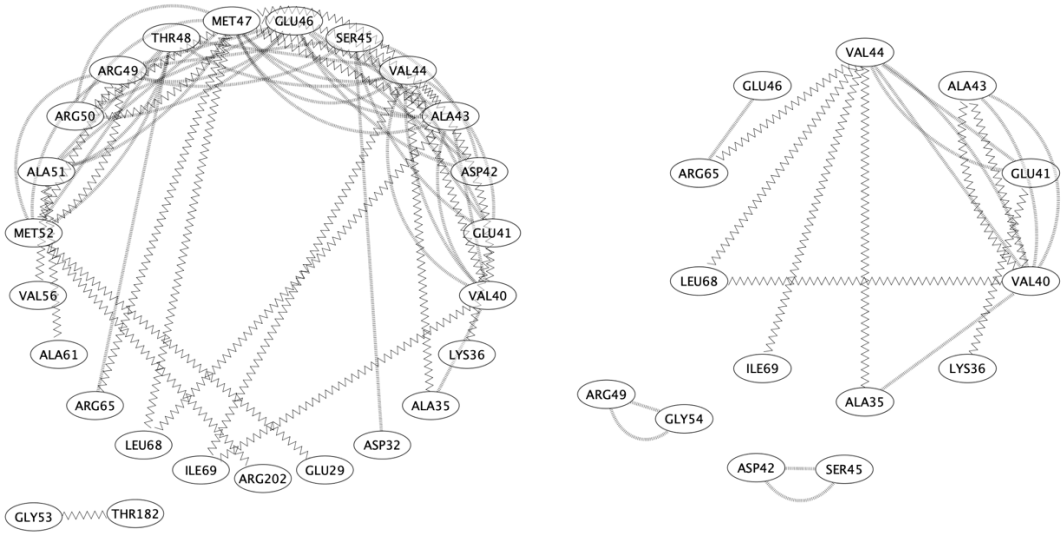

Chain A Chain B

Figure S5. Interaction networks depicting Hbonds (thick lines) and van der Waals interactions (zig-zag lines) involved by the residues 40 to 56 of the hPSP lid, as obtained by an analysis of the crystal chains A and B using RING (Piovesan et al., 2016). The RING results are displayed using the software Cytoskape (Shannon et al., 2003).

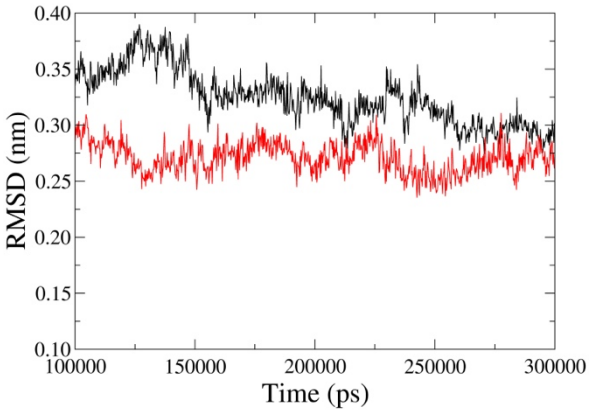

A/Ca/PSer (black), A_w/Ca/PSer (red)

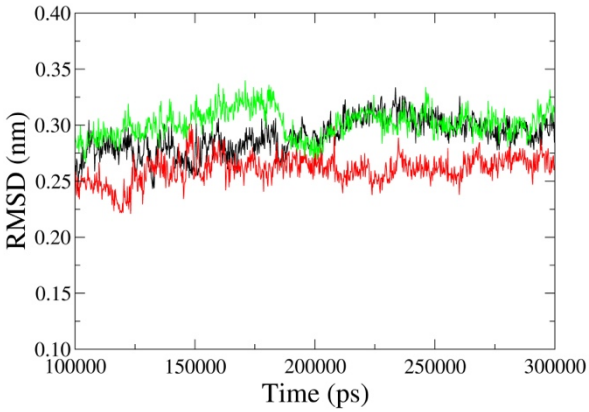

A_c/Mg/PSer (black), A_{cw}/Mg/PSer (red), A/Mg/PSer (green)

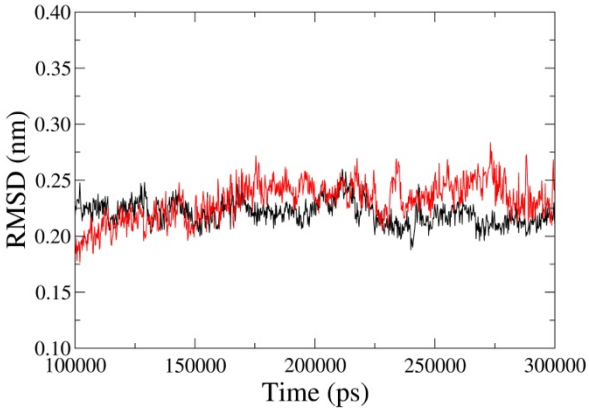

A_c/Mg (black), A_{cw}/Mg (red)

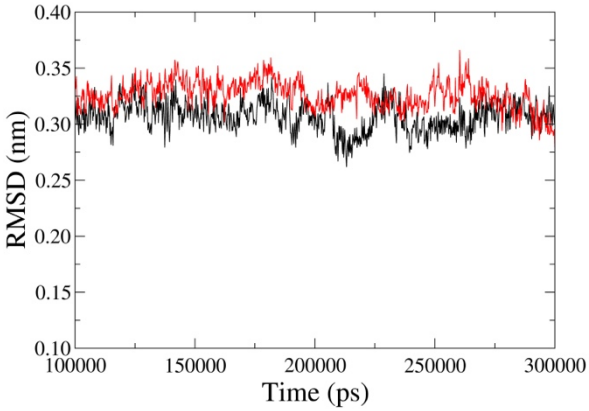

B/Ca (black), B/Mg (red)

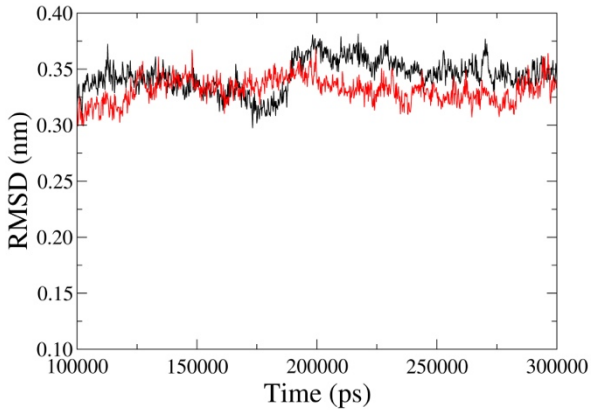

B/Ca/PSer (black), B/Mg/PSer (red)

Figure S6. RMSD of the solvated hPSP enzymes calculated versus their start conformation, as obtained from the last 200 ns of MD trajectories at 300 K and 1 bar.

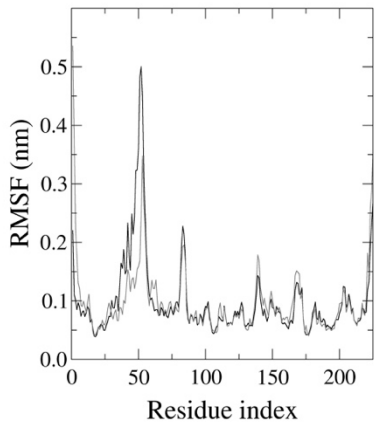

(a) A/Ca/PSer (black), A_w/Ca/PSer (grey)

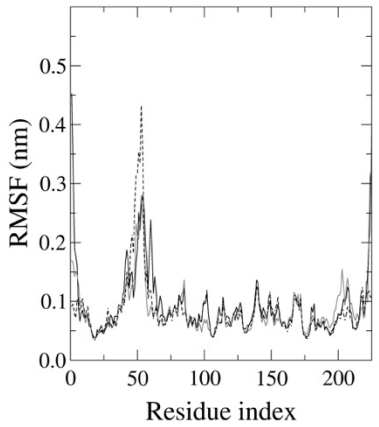

(b) A_c/Mg/PSer (black), A_{cw}/Mg/PSer (grey), A/Mg/PSer (dashed)

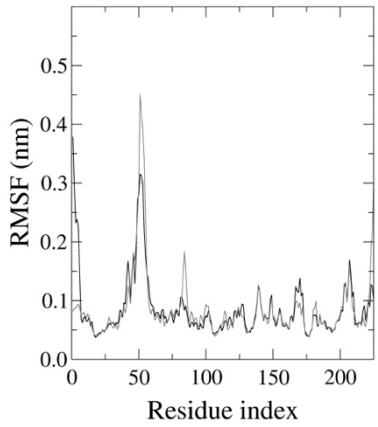

(c) A_c/Mg (black), A_{cw}/Mg (grey)

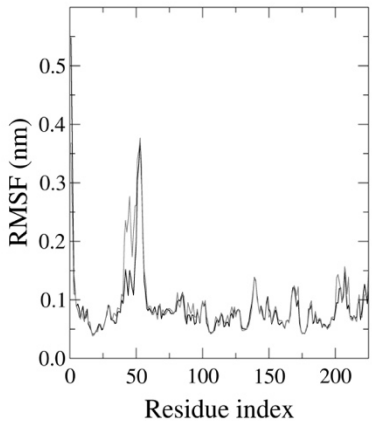

(d) B/Ca (black), B/Mg (grey)

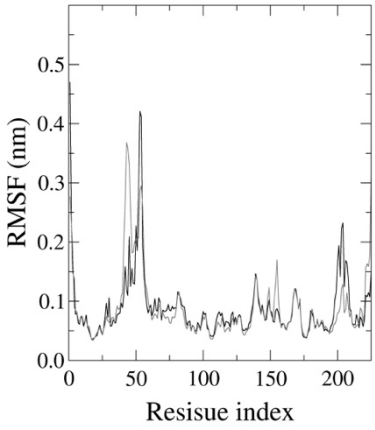

(e) B/Ca/PSer (black), B/Mg/PSer (grey)

Figure S7. RMSF of the hPSP Cα atoms as calculated from the last 200 ns of MD trajectories at 300 K and 1 bar.

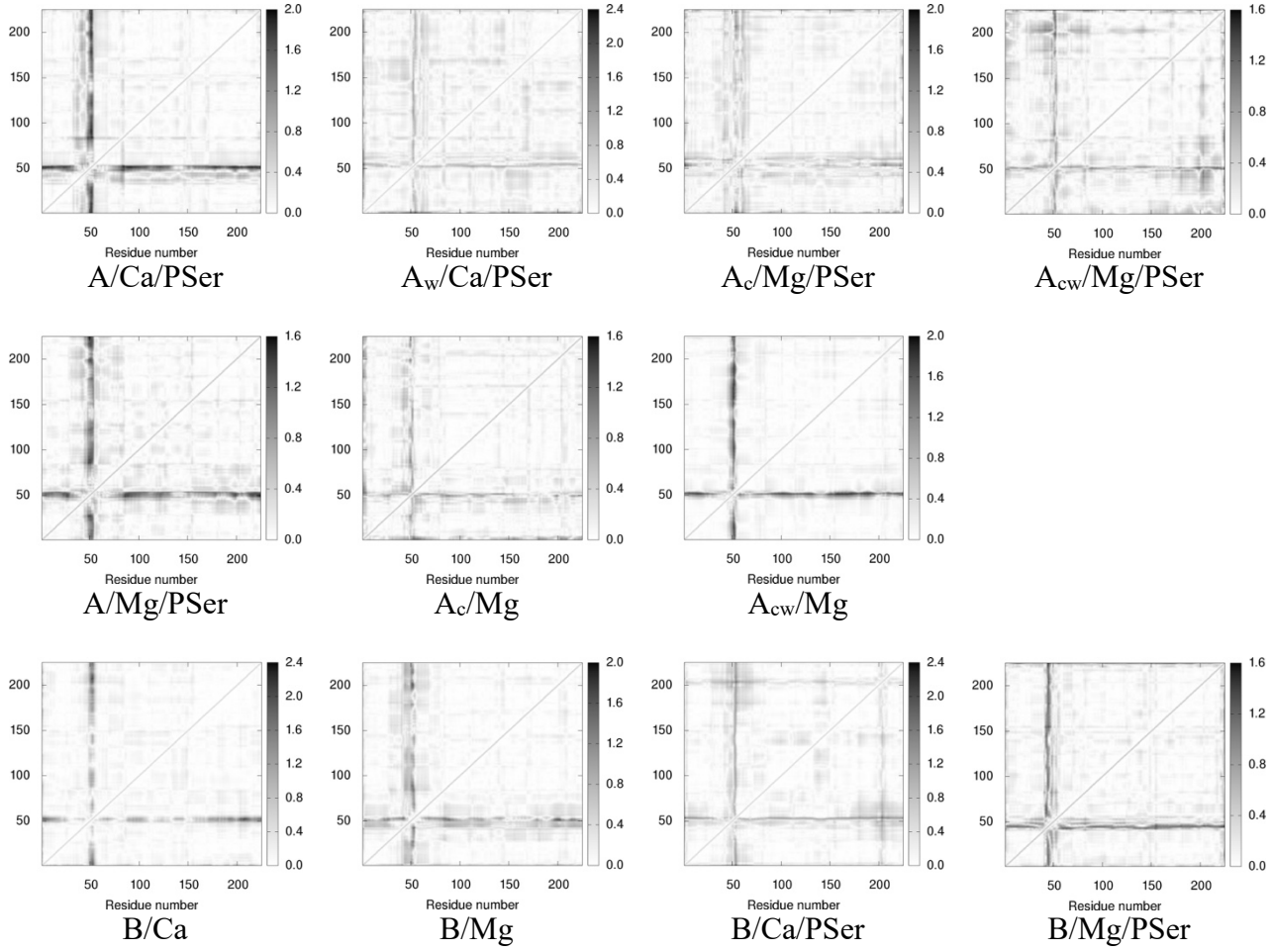

Figure S8a. hPSP $|\kappa_{ij}.\Delta d_{ij}|$ maps calculated using the first PC of the last 200 ns of MD trajectories at 300 K and 1 bar.

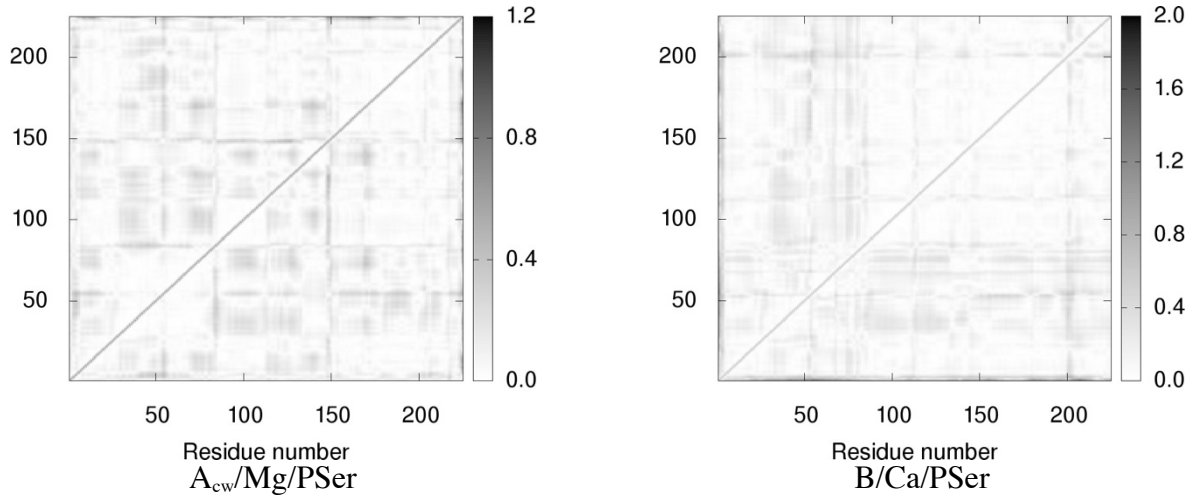

A_{cw}/Mg/PSer
Last 100 ns of the production stage

B/Ca/PSer
Last 75 ns of the production stage

Figure S8b. hPSP $|\kappa_{ij}.\Delta d_{ij}|$ maps calculated using the first PC obtained for a limited period of time of MD trajectories at 300 K and 1 bar.

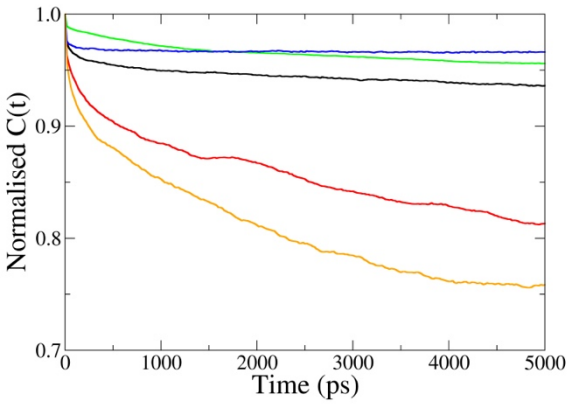

A/Ca/PSer (black), A_w/Ca/PSer (red), A_c/Mg/PSer (green), A_{cw}/Mg/PSer (blue), A/Mg/PSer (orange)

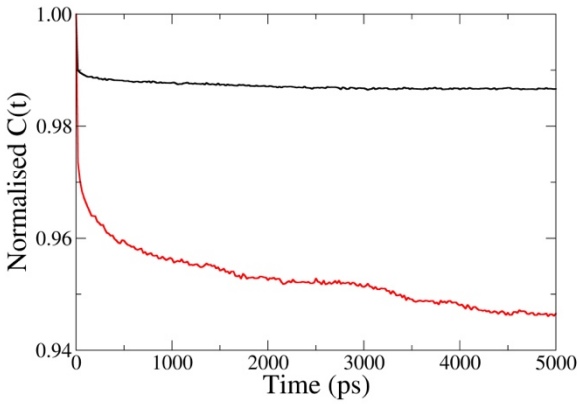

B/Ca/PSer (black), B/Mg/PSer (red)

Figure S9. First Legendre polynomial orientation autocorrelation function of the substrate PSer as obtained from the last 200 ns MD simulations at 300 K and 1 bar. Correlation times are reported in the Table below.

	τ (10^5 ps)
A/Ca/PSer	2.8
A_w/Ca/PSer	0.5
A_c/Mg/PSer	2.6
A_{cw}/Mg/PSer	38.6
A/Mg/PSer	0.3
B/Ca/PSer	40.7
B/Mg/PSer	3.8

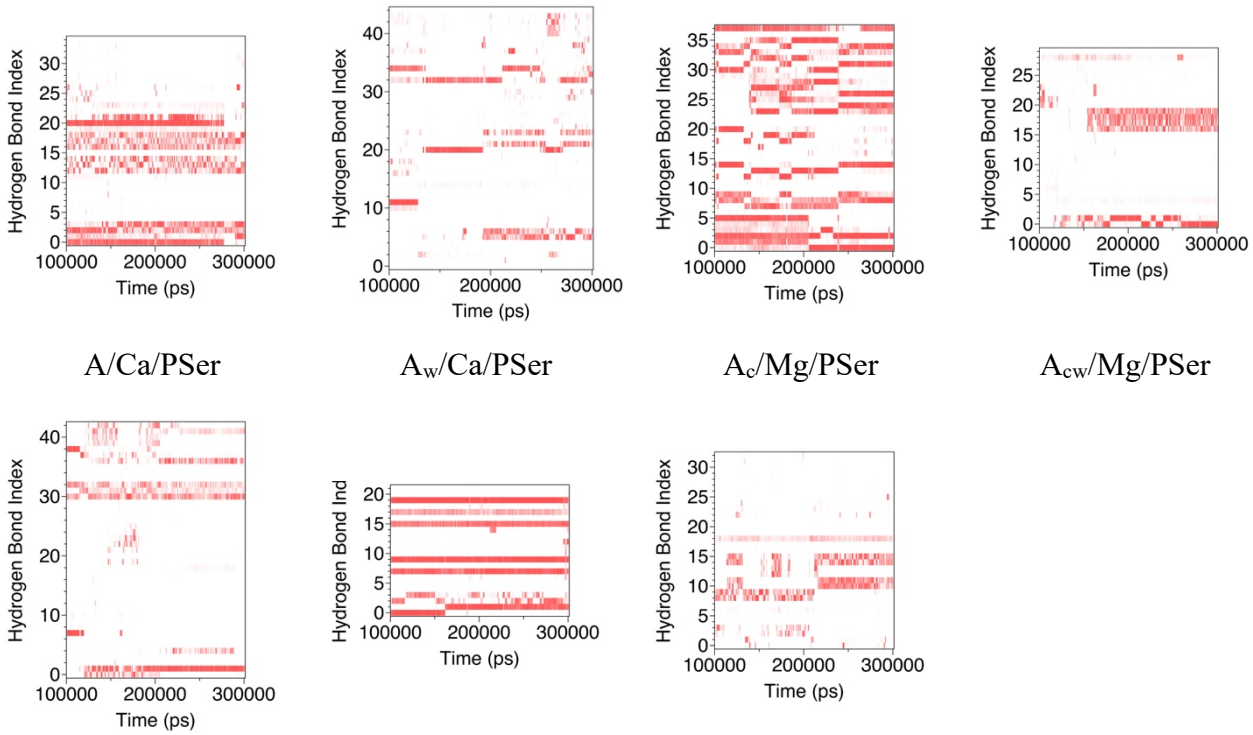

Figure S10. PSer-hPSP hydrogen bond maps as obtained from the last 200 ns of MD simulations at 300 K and 1 bar.

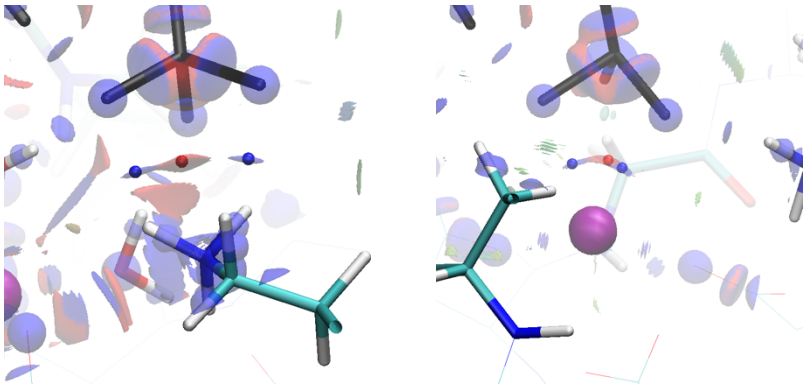

(b) Salt bridge PSer(phosphate)-Lys158 A/Mg/PSer

(c) Electrostatic PSer(phosphate)-Ion A_w/Ca/PSer

Figure S11. PSer (black sticks), selected passes (blue spheres) and pales (red spheres) superimposed to the 0.3 $e^{-1/3}$ isocontour of the RDG (negative (blue) and positive (red) transparent isosurfaces).

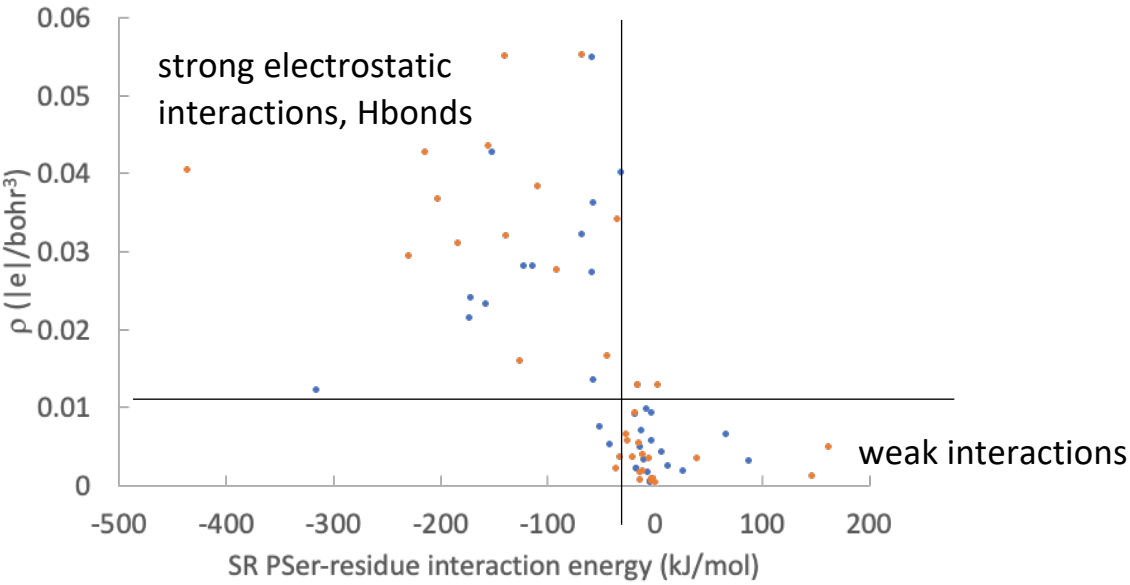

Figure S12. ED magnitude of the passes as a function of the corresponding SR interaction energy PSer-hPSP residue. Ca^{++}-dependent systems (blue), Mg^{++}-dependent systems (orange). See Table S10 for additional details. Extremely low SR interaction energies, below -10^3 kJ/mol, are not included in the Figure for the sake of clarity.

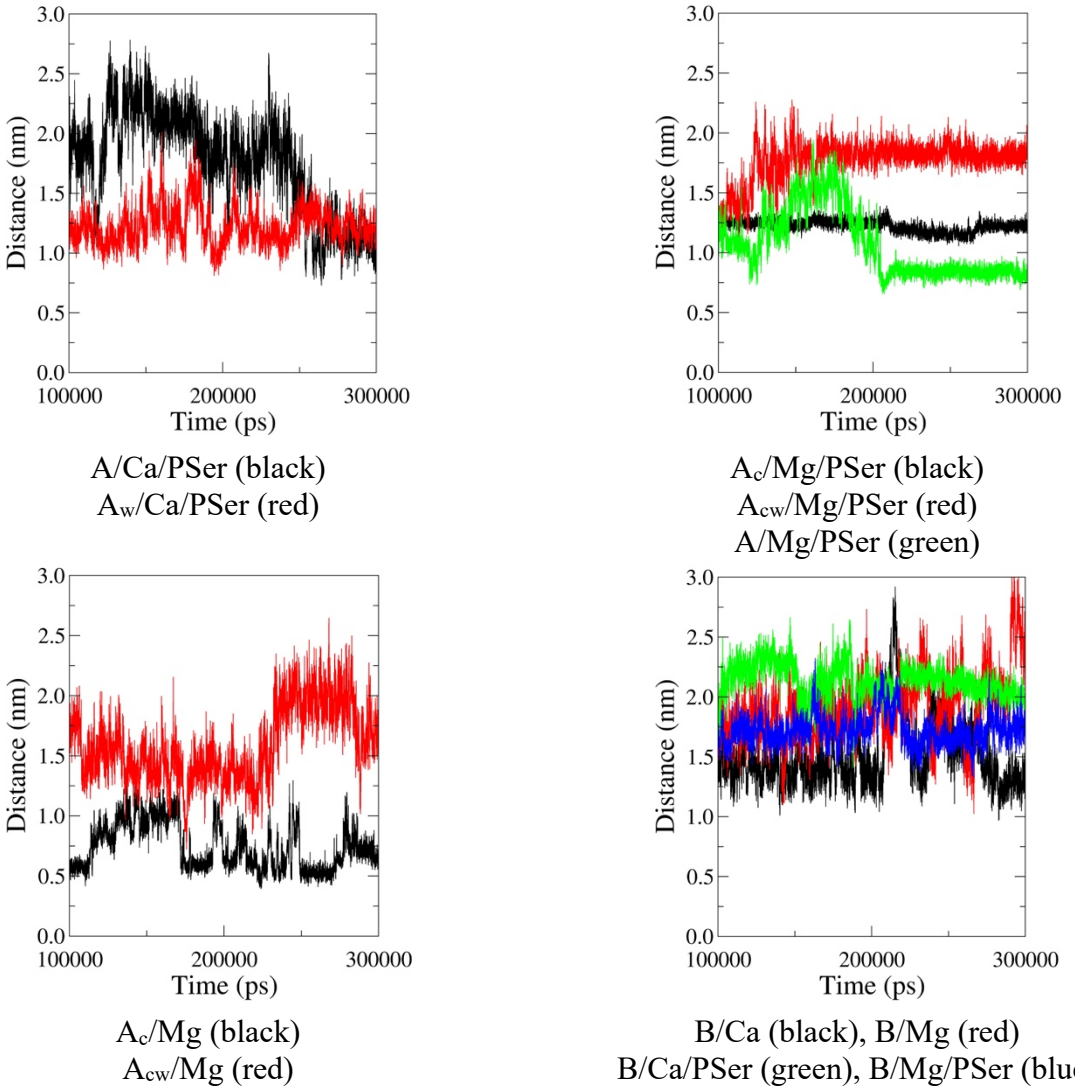

Figure S13. Distance profiles Cα52-Cα202 as obtained from the last 200 ns of MD simulations at 300 K and 1 bar.

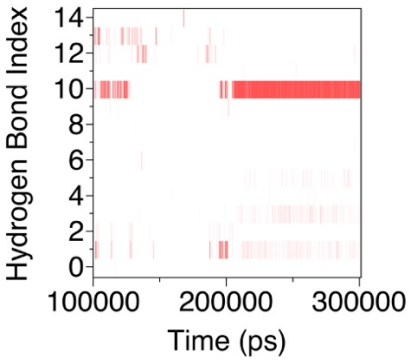

Figure S14. Profile of the hydrogen bonds occurring between amino acid sequences 50-55 and 202-206 for the system A/Mg/PSer as obtained from the last 200 ns of the MD simulation at 300 K and 1 bar.

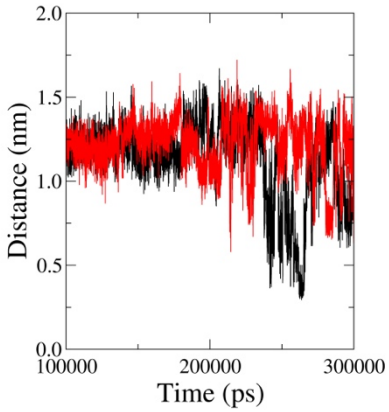

A/Ca/PSer (black); A_w/Ca/PSer (red)

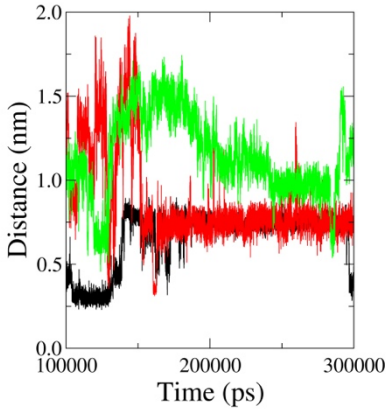

A_c/Mg/PSer (black); A_{cw}/Mg/PSer (red)
A/Mg/PSer (green)

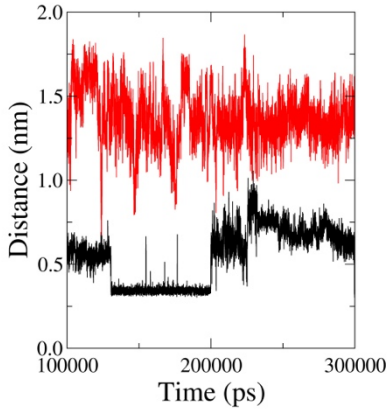

A_c/Mg (black); A_{cw}/Mg (red)

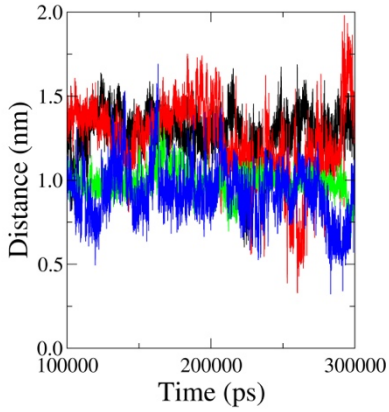

B/Ca (black); B/Mg (red)
B/Ca/PSer (green); B/Mg/PSer (blue)

Figure S15. Profiles of the minimum distance between CZ of Arg49 or Arg50 and Glu29, as obtained from the last 200 ns of MD simulations at 300 K and 1 bar.

References

Besler B. H., Merz K. M. Jr. & Kollman P. A. (1990) Atomic charges derived from semiempirical methods. *Journal of Computational Chemistry*, *11*(4):431-439.

Borodin O. & Smith G. D. Force field fitting toolkit. The University of Utah. http://www.eng.utah.edu/~gdsmith/fff.html. (last accessed 26 Aug. 2009).

Darré L., Tek A., Baaden M. & Pantano S. (2012). Mixing atomistic and coarse grain solvation models for MD simulations: Let WT4 handle the bulk. *Journal of Chemical Theory and Computation*, *8*(10):3880-3894.

Darré L., Machado M. R., Brandner A. F., González H. C., Ferreira S. & Pantano S. (2015). SIRAH: A structurally unbiased coarse-grained force field for proteins with aqueous solvation and long-range electrostatics. *Journal of Chemical Theory and Computation*, *11*(2),723-739.

Frisch M. J., Trucks G. W., Schlegel H. B., Scuseria G. E., Robb M. A., Cheeseman J. R., Scalmani G., Barone V., Mennucci B., Petersson G. A., Nakatsuji H., Caricato M., Li X., Hratchian H. P., Izmaylov A. F., Bloino J., Zheng G., Sonnenberg J. L., Hada M., Ehara M., Toyota K., Fukuda R., Hasegawa J., Ishida M., Nakajima T., Honda Y., Kitao O., Nakai H., Vreven T., Montgomery J. A. Jr., Peralta J. E., Ogliaro F., Bearpark M., Heyd J. J., Brothers E., Kudin K. N., Staroverov V. N., Kobayashi R., Normand J., Raghavachari K., Rendell A., Burant J. C., Iyengar S. S., Tomasi J., Cossi M., Rega N., Millam J. M., Klene M., Knox J. E., Cross J. B., Bakken V., Adamo C., Jaramillo J., Gomperts R., Stratmann R. E., Yazyev O., Austin A. J., Cammi R., Pomelli C., Ochterski J. W., Martin R. L., Morokuma K., Zakrzewski V. G., Voth G. A., Salvador P., Dannenberg J. J., Dapprich S., Daniels A. D., Farkas O., Foresman J. B., Ortiz J. V., Cioslowski J. & Fox D. J. (2009). Gaussian 09, Revision A.02, Gaussian, Inc., Wallingford CT.

Gonzáles H. C., Darré L. & Pantano S. (2013). Transferable mixing of atomistic and coarse-grained water models. *The Journal of Physical Chemistry B*, *117*(46),14438-14448.

Haufroid M., Mirgaux M., Leherte L. & Wouters J. (2019). Crystal structures and snapshots along the reaction pathway of human phosphoserine phosphatase. *Acta Crystallographica D*, *75*,592-604.

Hess B., Kutzner C., van der Spoel D. & Lindahl E. (2008). GROMACS 4: Algorithms for highly efficient, load-balanced, and scalable molecular simulationI *Journal of Chemical Theory and Computation*, *4*(3),435-447.

Homeyer N., Horn A. H. C., Lanig H. & Sticht H. (2006). AMBER force-field parameters for phosphorylated amino acids in different protonation states: phosphoserine, phosphothreonine, phosphotyrosine, and phosphohistidine. *Journal of Molecular Modeling*, *12*(3),281-289.

Humphrey W., Dalke A. & Schulten K. (1996). VMD - Visual Molecular Dynamics. *Journal of Molecular Graphics*, *14*(1),33-38.

Ichiye T. & Karplus M. (1991). Collective motions in proteins: A covariance analysis of atomic fluctuations in Molecular Dynamics and normal mode simulations. *Proteins*, *11*(3),205-217.

Leherte L. (2004). Hierarchical description of protein structure fragments obtained from analyses of promolecular electron density distributions. *Acta Crystallographica A*, 60,1254-1265.

Leherte L. (2016). Reduced point charge models of proteins: Assessment based on molecular dynamics simulations. *Molecular Simulation*, *42*(4):289-304.

Lindorff-Larsen K., Piana S., Palmo K., Maragakis P., Klepeis J. L., Dror R. O. & Shaw D. E. (2010). Improved side-chain torsion potentials for the Amber ff99SB protein force field. *Proteins*, *78*(8),1950-1958.

López-Blanco J. R., Aliaga J. I., Quintana-Ortí E. S. & Chacón P. (2014) iMODS: Internal coordinates normal mode analysis server. *Nucleic Acids Research*, *42*,W271-276. http://imods.chaconlab.org/ (last accessed 22 Sept. 2019).

Machado M. Tutorial 2. SIRAH forcefield in GROMACS, hybrid solvation: Plugging SIRAH solvent to your atomistic system. https://training.vi-seem.eu/images/trainingMaterial/LifeSciences/Tutorial_2_sirah4gmx.pdf (last accessed 27 Jun. 2018).

Peeraer Y., Rabijns A., Collet J.-F., Van Schaftingen E. & De Ranter C. (2004). How calcium inhibits the magnesium-dependent enzyme human phosphoserine phosphatase. *European Journal of Biochemistry*, *271*(16),3421-3427.

Pedretti A., Villa L. & Vistoli G. (2004). VEGA - An open platform to develop chemo-bio-informatics applications, using plug-in architecture and script programming. *Journal of Computational Aided Molecular Design*, *18*(3),167-173.

Piovesan D., Minervini G. & Tosatto S. C. E. (2016). The RING 2.0 web server for high quality residue interaction networks. *Nucleic Acids Research*, *44*,W367-374.

Pronk S., Páll S., Schulz R., Larsson P., Bjelkmar P., Apostolov R., Shirts M. R., Smith J. C., Kasson P. M., van der Spoel D., Hess B. & Lindahl E. (2013). GROMACS 4.5: A high-throughput and highly parallel open source molecular simulation toolkit. *Bioinformatics*, *29*(7),845-854.

Ray B. D. (2009). Topolbuild 1.3, IUPUI Physics Dept., Indianapolis IN. http://www.gromacs.org/Downloads/User_contributions/Other_software (last accessed 12 Dec. 2018).

Ryu J., Lee M., Cha J., Laskowski R. A., Ryu S. E. & Kim D.-S. (2016). BetaSCPWeb: side-chain prediction for protein structures using Voronoi diagrams and geometry prioritization. *Nucleic Acids Research*, *44*,W416-W423.

Salentin S., Schreiber S., Haupt V. J., Adasme M. F. & Schroeder M. (2015). PLIP: fully automated protein–ligand interaction profiler. *Nucleic Acids Research*, *43*(W1),W443-W447.

Schrödinger, LLC (2014). The PyMOL Molecular Graphics System, Version 1.7.4.

Shannon. P., Markiel A., Ozier O., Baliga N. S., Wang J. T., Ramage D., Amin N., Schwikowski B., & Ideker T. (2003). Cytoscape: A software environment for integrated models of biomolecular interaction networks. *Genome Research*, *13*(11),2498-2504.

Singh U. C. & Kollman P. A. (1984). An approach to computing electrostatic charges for molecules. *Journal of Computational Chemistry*, *5*(2),129-145.

Steinbrecher T., Latzer J. & Case D. A. (2012). Revised AMBER parameters for bioorganic phosphates. *Journal of Chemical Theory and Computation*, *8*(11),4405-4412.